

Detection of oligonucleotide hybridization at femtomolar level and sequence-specific gene analysis of the *Arabidopsis thaliana* leaf extract with an ultrasensitive surface plasmon resonance spectrometer

Fayi Song, Feimeng Zhou*, Jun Wang, Nongjian Tao¹, Jianqiao Lin, Robert L. Vellanoweth, Yvonne Morquecho and Janel Wheeler-Laidman

Department of Chemistry and Biochemistry, California State University, Los Angeles, 5151 State University Drive, Los Angeles, CA 90032, USA and ¹Department of Electrical Engineering, Arizona State University, Tempe, AZ 85287, USA

Received December 28, 2001; Revised May 1, 2002; Accepted May 31, 2002

ABSTRACT

A flow-injection (FI) device is combined, through the use of a low-volume (4 μ l) flow cell, with an ultrasensitive surface plasmon resonance (SPR) spectrometer equipped with a bi-cell photodiode detector. The application of this novel FI-SPR device for sequence-specific ultratrace analysis of oligodeoxynucleotides (ODNs) and polydeoxynucleotides was demonstrated. Self-assembled monolayers of ODN probes are tethered onto Au films with a mercaptohexyl group at the 3' ends. The FI-SPR provides a detection level (≤ 54 fM) 2–3 orders of magnitude lower than other SPR devices and compares well with several ultrasensitive detection methods for labeled DNA targets (e.g. fluorophore-tagged and radiolabeled DNA samples). The technique is also highly selective, since a 47mer ODN target with a single-base mismatch yielded a much smaller SPR signal, and a specific interaction was detected when the complementary target was present at 0.001% of the total DNA. The FI-SPR was extended to the measurement of two individual genes in a cDNA mixture transcribed from an *Arabidopsis thaliana* leaf mRNA pool. The greatly enhanced sensitivity not only obviates the necessity of DNA labeling, but also significantly reduces sample consumption, allowing direct quantification of low abundance mRNAs in cellular samples without amplification.

INTRODUCTION

Recent advances in developmental cell biology coupled with the rapid influx of genomic data have illuminated the need for highly sensitive methods of single gene expression analysis.

Typical biological tissues contain at least several different cell types, each with its own set of expressed genes that provide for that cell's function within the organism. In order to understand how a particular set of genes determines the functional fate of a cell type, it has become apparent that expression analysis within small samples of cells is critical. In addition, many genes are expressed at very low levels, including important regulatory genes such as those involved in transcription and signal transduction. The quantification of their expression has proven difficult owing to the limited sensitivity of the existing RNA/DNA detection methods.

The most common methods for the quantification of gene expression include northern blotting (1), ribonuclease protection and reverse transcription-polymerase chain reaction (RT-PCR) (2,3). The first two methods require 10–100 μ g of RNA and can detect single mRNAs at the 10^6 – 10^7 copy level (2,3). Such quantities can be easily isolated from bulk tissues, but if one has very small amounts of tissue or has a need to separate only certain cell types for analysis, northern blotting and ribonuclease protection techniques are not feasible. RT-PCR can theoretically amplify single molecules and thus could be useful for very small sample sizes (2,3). However, it requires considerable optimization of primer sets, and for an accurate quantification, concerns have been raised about differential amplification efficiencies of target and standard DNAs (4). Moreover, among all the methods, sample pretreatment or amplification tends to introduce contamination and/or prolongs the analysis time.

Alternative sequence-specific detection methods, such as optical (5–7) and electrochemical methods (8–13), quartz crystal microbalance (QCM) (14–21) and capillary electrophoresis coupled with fluorescence detection (22) have been recently developed. Many of these methods are either relatively insensitive without signal amplification [e.g. QCM (21)] or require prior labeling of the DNA sample with species that can give rise to the analytical signals (e.g. attaching an electroactive tag onto the DNA target). Among the various

*To whom correspondence should be addressed. Tel: +1 323 343 2390; Fax: +1 323 343 6490; Email: fzhou@calstatela.edu

techniques reported for sequence-specific DNA analysis, surface plasmon resonance (SPR) (23–26) has been shown to be a rapid and sensitive means (27,28) for the study of biomolecular reactions, such as DNA hybridization (28–36), protein–protein and DNA–protein interactions (37–40) and ligand–receptor binding (41). The high sensitivity of SPR in some cases obviates the need for labeling the DNA sample analyte, dramatically enhancing the sample throughput.

The two popular SPR detection schemes involve either the use of a photodetector to monitor the reflection of collimated light as a function of incident angle or the adoption of a linear diode array or a charge coupled device to detect the reflection of a converged light beam. Both approaches can achieve angular resolutions of $\sim 10^{-2}$ – 10^{-3} degrees under favorable experimental conditions. For example, on the commercial BIAcore SPR instrument (42), the rotary angle or intensity of the reflected light was directly measured with a resolution of $\sim 0.001^\circ$. While such an angular resolution results in a relatively high sensitivity, the sample detection levels are not as low as the aforementioned biochemical assays. For example, in oligodeoxynucleotide (ODN) hybridization analysis, most of the reported detection levels are still in the nanomolar or subnanomolar range (28,30,31,33–36,43). While the use of DNA-capped gold nanoparticles (29,37,38) or samples tagged with liposomes or latex particles in a sandwich assay format (40,44) has been noted to lower the detection levels to a few pmol, it is still challenging for such an approach to determine genes at low expression levels, especially when the amount of available sample is limited.

In this work, we combined a high-resolution SPR (45) with a flow injection (FI) device for sequence-specific analysis of label-free DNAs at an ultrasensitive level. The incorporation of a bi-cell photodiode detector to measure the shift of a sharp dark line (the SPR dip shift) (46) resulted in a much-improved angular resolution (10^{-4} – 10^{-5} degrees). A low-volume (4 μ l) flow cell was constructed and coupled with the SPR device through a six-port rotary valve. The ODN probes whose 3' ends are linked to a mercaptohexyl tether group (HS-ODNs) were anchored onto the sensor surface through the formation of self-assembled monolayers (SAMs). The analytical performance (e.g. sensitivity, selectivity and hybridization efficiency) of this FI–SPR device was assessed by comparing the results with previously reported studies. We show that our FI–SPR can detect ODNs of attomole (10^{-18} mol) quantities without sample derivatization or post-hybridization treatment for signal amplification. Finally, the application of our FI–SPR device to the detection of two specific genes in a small amount of *Arabidopsis thaliana* total leaf cDNA pool demonstrates that quantifying unlabeled DNA samples present in a complex matrix is highly feasible.

MATERIALS AND METHODS

Materials

EDTA, tris(hydroxymethyl)aminomethane hydrochloride (Tris–HCl), NaOH, NaCl and sodium citrate were obtained from Aldrich Chemicals. Ethidium bromide and guanidine isothiocyanate were purchased from Sigma. All of the HS-ODN probes and their complementary and mismatching

targets as well as the primer used for the RT–PCR experiment were acquired from Integrated DNA Technologies, Inc. (Coralville, IA). For evaluating the analytical performance of the FI–SPR instrument, a 30mer HS-ODN 5'-AGAGGATCCCCGGGTACCGAGCTCGAATTC(CH₂)₆SH-3', its complementary 47mer target 5'-GAATTCGAGCTCGGTA-CCCCGGGGATCCTCTACTGGCCGTCGTTTTAC-3' and two targets with single and six mismatching bases were used. These non-complementary targets, with their mismatching base(s) underlined, have the following sequences: 5'-GACTTCGAGCTCGGTACCCGGGGATCCTCTACTGGCCGTCGTTTTAC-3' and 5'-CTTGGAGAGCTCGGTACCCGGGGATCCTCTACTGGCCGTCGTTTTAC-3'. For the detection of the *A.thaliana* cDNAs, a 35mer probe, 5'-TCGGGTTTGCTGACAAGGAGTAATCTGGAATCTGG-(CH₂)₃SH-3' was used for the ascorbate peroxidase glyoxysome-bound (APx-cs2) gene, whereas the 35mer actin gene 5'-TGAGGCAGGTCCAGGAATCGTTCACAGAAAATGTT-(CH₂)₃SH-3' was employed as a control. We also utilized a probe that has one base mismatching the APx-cs2 gene, 5'-TCGGGTTTGCTGACAAGGAGTAATCTGGAATATGG-(CH₂)₃SH-3' to examine the sequence specificity. The solution preparation and probe immobilization follows our previously published procedures (18,47).

mRNA analysis by RT–PCR

Total RNA was extracted from *A.thaliana* leaves by homogenization of leaf tissue in its pre-bolt stage using guanidine isothiocyanate, followed by silica-gel-based micro spin column separation (Qiagen RNeasy). mRNA was isolated from total RNA by oligo-dT micro spin column (Qiagen Oligotex) and eluted into RNase free water. mRNA was quantified by spot-blot with ethidium bromide and analyzed for pixel density via Molecular Analyst (BioRad) software. cDNA was synthesized from mRNA using M-MLV reverse transcriptase (Gibco-BRL Superscript II) and an oligo-dT primer. The cDNA was subsequently used as a template for amplification via PCR using primers specific to the APx-cs2 and actin2 genes (30 cycles). Separate reactions with varying amounts of mRNA (1.0, 5.0, 10.0, 20.0 and 50.0 ng) were used for RT–PCR to determine whether there was a linear correlation between the amount of starting mRNA and eventual PCR product.

PCR kinetics

Aliquoted PCRs for both APx-cs2 and actin2 genes were set up and portions removed from the thermocycler at selected intervals (5, 10, 15, 20, 25 and 30 cycles). Each portion was run on 0.7% agarose, stained with ethidium bromide and then analyzed for pixel density using the Molecular Analyst software.

Primer design

Actin2 primers were designed from the *Arabidopsis* sequence (NCBI accession no. U37281) to amplify a 1137 bp region (from cDNA) of the *A.thaliana* actin2 gene. APx-cs2 primers were designed from the *Arabidopsis* sequence (NCBI accession no. X98276) to amplify a 563 bp region (from cDNA) of the APx-cs2 gene.

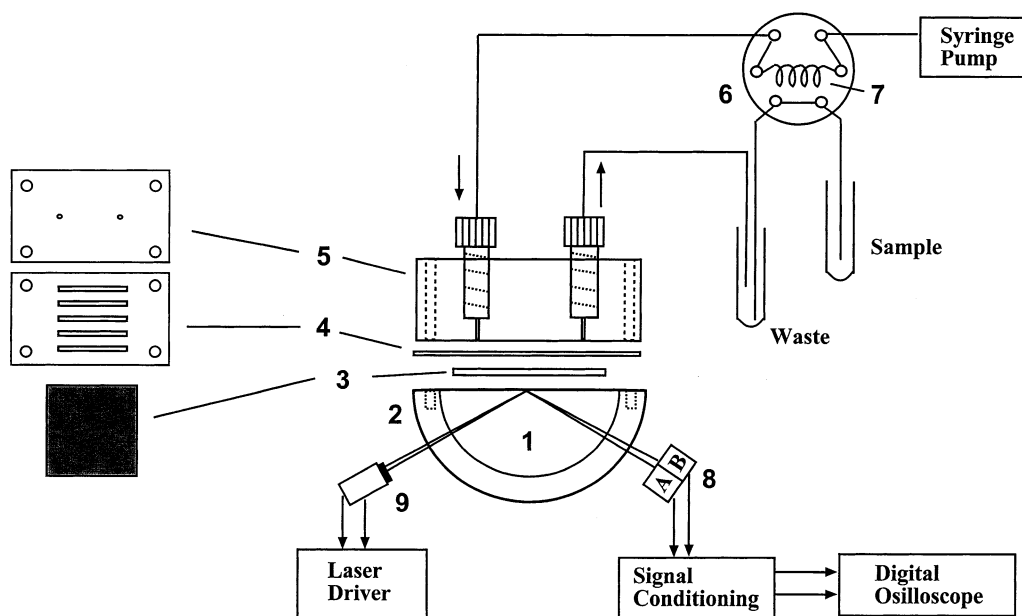


Figure 1. Side (cut-off) view of the FI-SPR setup. 1, prism; 2, prism holder; 3, glass slide coated with a thin Au film; 4, teflon separation gasket; 5, acrylic flow cell containing four holes for the attachment to the prism holder; 6, six port valve; 7, sample loop; 8, bi-cell photodetector; 9, diode laser with a collimator and a focusing lens. The face view of the Au/glass slide, the gasket and the flow cell is shown on the left of the diagram.

Fabrication of Au-coated glass slides

BK7 glass cover slides (Fisher) were thoroughly rinsed with acetone, ethanol and deionized water. Upon drying, they were coated with 50-nm-thick gold films. Two different thin metal film coaters, a sputtering coater (Model 108, Kurt J. Lester Corp., Clairton, PA) and an ion beam coater (Model 681, Gatan Inc., Pleasanton, CA) were employed for the Au film deposition. The films fabricated with the ion beam coater were found to be more uniform than those prepared with the sputtering coater, because the glass substrates were rotated during the coating process under a higher vacuum (10^{-6} torr versus 10^{-3} torr in the chamber of the sputtering coater). While the ion beam coater produces films of better quality, which ultimately lead to results with a more satisfactory reproducibility (see Results), the set-up and maintenance expenses and the cost per Au-coated slide (\$5–10) are much higher than those fabricated with the sputtering coater. The films deposited using the sputtering coater have an average cost of ~\$1 per slide and yield SPR data with a satisfactory precision (<9% relative standard deviation, *vide infra*). Therefore, except for the study about the effect of Au film uniformity on the precision of the SPR data, Au films formed with the sputtering coater were used throughout most of this work. The low cost and the ease of preparation render such films as disposable sensors.

Instrumentation

Figure 1 is the schematic diagram of the FI-SPR setup. Light from a 10 mW diode laser ($\lambda = 635$ nm, Sanyo) undergoes a total internal reflection in the BK7 prism (Melles Griot, Irvine, CA). The reflected light from the 50-nm-thick Au film deposited on top of a 2 nm Cr thin film is detected with a bi-cell photodiode detector (Hamamatsu Corp., Model S2721-02) that is mounted on a precision translation/rotation stage

(Melles-Griot). Before each measurement the prism was rotated so that there was a dark line located at the center of the laser spot. The dark line is due to the absorption of the light by the surface plasmon, which occurs at the angle of resonance. The reflected light falling onto the two cells (A and B) of the photodetector was then balanced by adjusting the photodetector position with the translation stage until the differential, $A - B$, approached zero. Both the differential ($A - B$) and the sum ($A + B$) signals were measured by a digital oscilloscope (Yokogawa, DL1520I). The ratio of the differential to sum signals, which is linearly proportional to the SPR angular shift, was obtained numerically by dividing $A - B$ with $A + B$. The flow cell was attached to the prism holder through four threaded holes. The homemade acrylic flow cell has a cross-flow configuration with an internal volume of ~4 μ l. The inlet of the cell is connected to a six-port rotary valve (Valco Instruments Co., Houston, TX). Five channels on the separation gasket with equal spacing in between were carved to allow multiple uses of each Au film. The purpose for multiple usages of the same Au film is two-fold: (i) the sample throughput should be improved because a smaller number of Au films will be needed for a given number of analyses; and (ii) the precision should also be improved because variations in the thickness and surface morphology of Au films deposited onto different glass slides are eliminated. For each analysis, the sample was preloaded into a 100 μ l loop with a microsyringe (Fisher). Upon injection, the sample solution was introduced into the flowing buffer solution and subsequently delivered to the flow cell by a syringe pump (Harvard Apparatus).

Procedures

DNA probe immobilization. Prior to the SPR measurement, each Au film was annealed in a hydrogen flame to reduce

surface contamination. The formation of the HS-ODN SAMs at the sensor surface can be accomplished by immersing the Au film in a 0.28 μM HS-ODN probe solution for 4 h (18).

DNA target hybridization. For detecting both the oligonucleotide targets and the cDNAs transcribed from the mRNAs in the *A.thaliana* leaf extracts, TE solutions (10 mM Tris-HCl and 1 mM EDTA) containing 0.1 M NaCl were used as the hybridization buffer. Such an ionic strength has been shown to be sufficient for the hybridization reactions to occur at a high efficiency at surfaces (11,18,19,48,49). We found that the stability of the signal is highly dependent on the ambient temperature (46). Therefore, the instrument was housed in a well ventilated room with the ambient temperature regulated at 28°C. In addition, all the solutions freshly prepared or preserved in a freezer or refrigerator were left in the room for a prolonged period of time to allow the solution temperature to equilibrate to the ambient value. Although the hybridization would proceed at a faster rate at a temperature higher than room temperature, we did not attempt to heat the sensing device and/or the flow cell because of the well known high variability of SPR signals caused by the temperature fluctuation (46). As shown by other SPR studies (23,27,30,34,50,51) and the results presented below, our approach and setup produce satisfactory results in terms of the hybridization kinetics and efficiency.

The TE/NaCl carrier solution was introduced through the injection valve at a flow rate of 25 $\mu\text{l}/\text{min}$. Once a stable baseline was established, the valve position was switched to the inject position to divert the analyte solution to the flow cell. It takes ~ 70 s for the injected sample to travel from the loop to the cell. The cell content will be completely replaced by the carrier solution 320 s after the injection from a 100 μl loop. Therefore, the total analysis time per sample is ~ 5 –6 min. Six different concentrations of a 47mer (0.054, 0.11, 0.18, 0.36, 1.2 and 1.8 μM) were measured. All of the hybridization experiments were conducted at room temperature. At least three replicate measurements were made for all of the 47mer target solutions and the various samples containing *Arabidopsis* cDNAs.

RESULTS

DNA probe immobilization

We first studied the immobilization of a 30mer HS-ODN onto an Au surface in order to compare the probe surface coverage and hybridization with published reports based on other analytical and/or surface methods (18,30,52–55). It is well established that HS-ODN can readily adsorb onto Au surfaces, but do not form well ordered SAMs due to the non-specific interactions between the DNA bases and the Au surface (18,30,35,52–55). It has been shown that ODNs with relatively long strands tend to pack less densely than the shorter ODNs [e.g. ≤ 24 bases (52)].

Figure 2 shows FI-SPR responses (dip shifts in unit of degrees) to the injections of 100 μl of 0.28 μM (curve A) and 2.8 nM (curve B) of a 30mer HS-ODN probe that is complementary to the 47mer target used for the model study. As can be seen, the time lapse between the injection and the initial change of SPR dip shift correlates well with the time

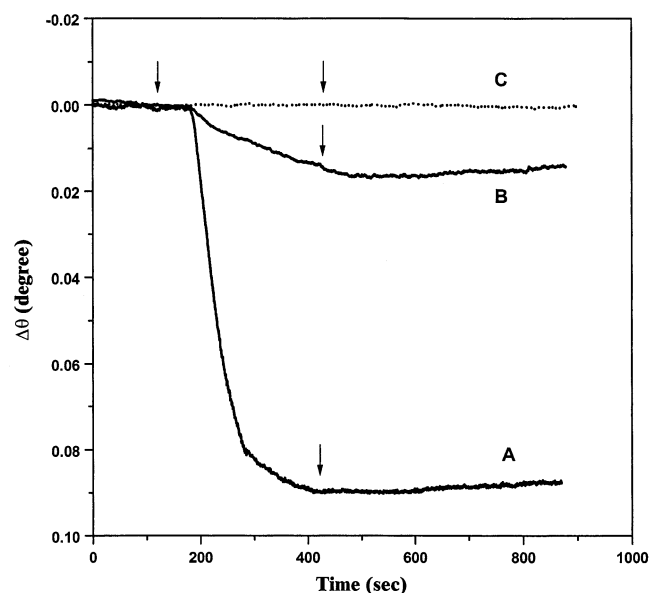


Figure 2. Time-resolved SPR responses to the injections of 100 μl of a TE solution containing 0.28 μM (curve A) and 2.8 nM of 30mer HS-ODN (curve B) probe solutions. An injection of 100 μl of a TE solution into the SPR cell (curve C) is also shown. Arrows indicate the times when injections were performed and when the injected samples were completely replaced by the carrier solution.

needed for the injected sample to reach the sensor surface. As soon as the probe solution enters the cell, a drastic dip shift (at ~ 180 s in Fig. 2) was registered, suggesting that the adsorption of the HS-ODN is instantaneous. The attainment of the final dip value (0.09°) was reached at ~ 420 s. The dip shift remained steady even after the cell contents were replaced by the buffer solution, indicating that the probe adsorption was irreversible.

In an effort to quantify the maximum surface coverage of the HS-ODN, we performed multiple injections of the 0.28 μM probe solution until the SPR dip shift became constant. The cumulative amount of probe adsorption was calculated from the overall dip shift (data not shown). The overall dip shift (0.1°) corresponded to an average surface coverage of 11% based on the comparison with full surface coverage. If the theoretical ODN probe surface density (6×10^{13} molecules/ cm^2) (52) is used, this average surface coverage corresponds to a value of $\sim 6 \times 10^{12}$ molecules/ cm^2 . We also carried out multiple injections of the 35mer APx-cs2 probe solution and found the average surface coverage to be 10%. The average surface coverage of these HS-ODN probes deduced from the FI-SPR measurements is important for calculating the hybridization efficiencies associated with ODN targets and the cDNA targets in the *A.thaliana* samples.

Hybridization of oligonucleotide targets at ultratrace levels

In order to estimate the detection levels of our FI-SPR for DNA analysis, we measured dip shifts as a function of the target concentration. The Au surface immobilized with the 30mer HS-ODN was first applied to the SPR detection of hybridization to a complementary 47mer target. Curves A and B in Figure 3 depict the SPR dip shifts recorded with the

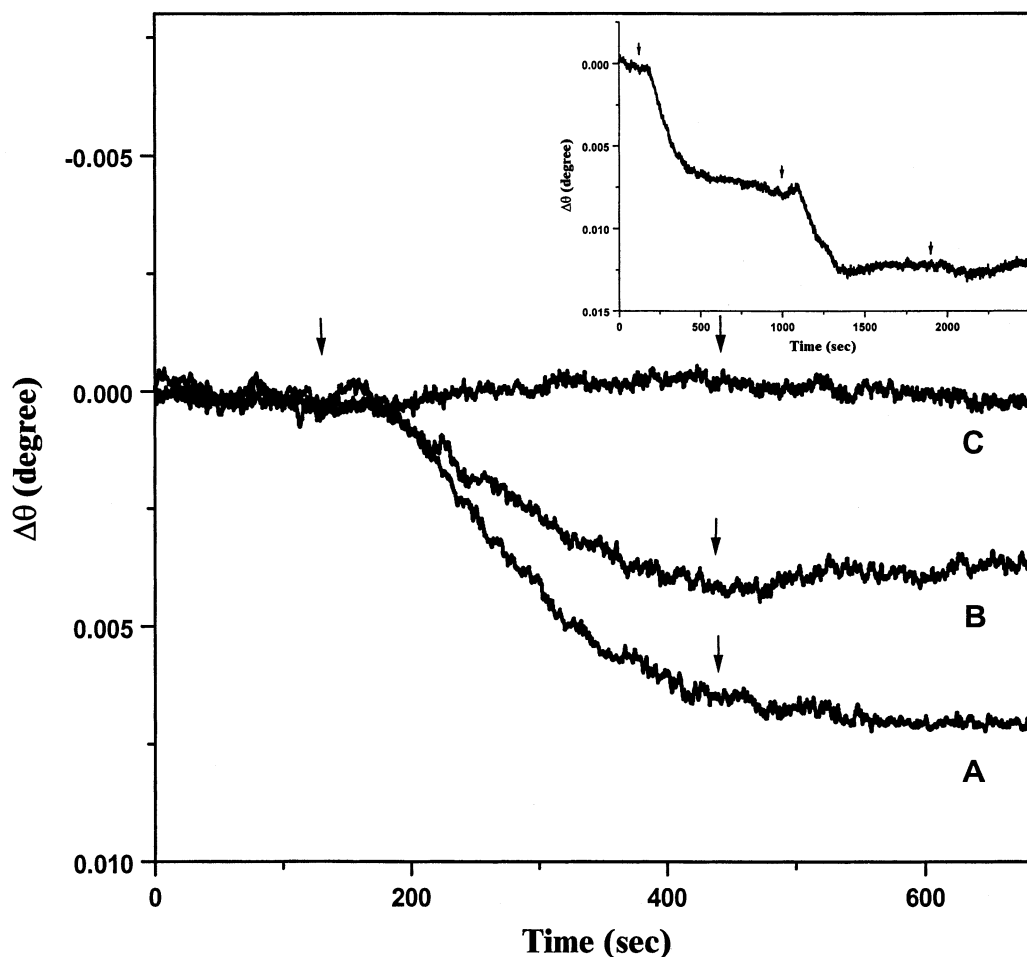


Figure 3. Time-resolved SPR responses at the 30mer HS-ODN probe-modified Au films to the injections of 100 μ l of 0.18 pM (curve A) and 0.054 pM (curve B) solutions containing the complementary 47mer target. The injection of the target solution (18 pM) into the flow cell housing a bare Au film is shown as curve C. The inset shows three consecutive injections of 100 μ l of the complementary target solution (0.18 pM). Arrows indicate the times when injections were performed and when injected samples were completely replaced by the carrier solution.

injections of 100 μ l of 0.18 and 0.054 pM of a 47mer target into the cell housing the 30mer-covered Au films, respectively. As a control, the SPR response to the injection of the 47mer complementary target solution into the flow cell housing a bare Au film was also monitored (curve C). The absence of any SPR dip shift indicates that any non-specific ODN adsorption on the bare Au film substrate was not detectable. Therefore, the dip shifts in curves A and B must have originated from target adsorption through the duplex formation with the immobilized probes.

We conducted consecutive injections of the 0.18 pM ODN target solution to determine the total amount of target hybridizable at the sensor surface. As evidenced by the inset of Figure 3, the essentially indistinguishable SPR dip shift after the third injection suggests that most of the probes available for hybridization had been consumed. The average surface coverage of the duplex DNA molecules calculated on the basis of the overall SPR dip shift was $\sim 1\%$. This corresponds to hybridization with $\sim 9\%$ of the probe molecules available at the surface. Levicky *et al.* (54) estimated $\leq 10\%$ hybridization based on small neutron reflectivities and Piscevic *et al.* (35) reported 9% hybridization

of a 10-base-long HS-ODN. Thus our value is in good agreement with the previously reported results. This is also consistent with our recent FI-QCM and atomic force microscopy (AFM) measurements, which showed a 17% hybridization efficiency for a 17mer target (48).

The SPR dip shift was next measured as a function of the target concentration (Fig. 4). The relative standard deviations (% RSD values) are all $< 9\%$ which are considered to be acceptable among established analytical techniques (56). While any slight variation in solution compositions or ambient temperature could introduce errors to the results, the uniformity and the thickness of the Au films appear to have the most profound effect. Such a contention is drawn from our observation that the precision of the data collected from different Au films was slightly lower than that recorded at several locations of the same film (via switching to different channels on the gasket, *vide supra*). To further verify this contention, we compared the precision of the results acquired at films fabricated with the sputtering coater with that obtained at films produced with an ion beam coater, and found that the latter precision was generally better. For example, for the measurement of a sample containing 0.18 pM 47mer target,

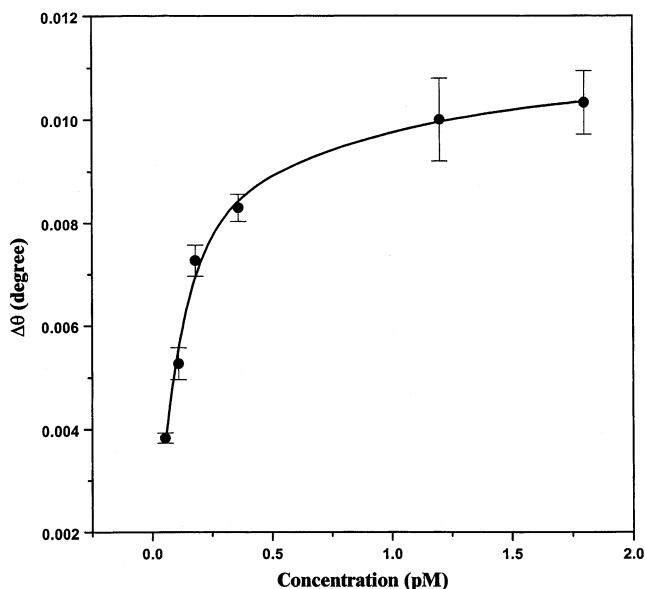


Figure 4. SPR dip shift plotted as a function of the target. The six target concentrations are 0.054, 0.11, 0.18, 0.36, 1.2 and 1.8 pM, respectively. The absolute uncertainties were computed from at least three replicate measurements and shown as the error bars.

the relative standard deviation was improved from 8.8% (sputtered films) to 4.5% (films formed with the ion beam coater). Despite such a palpable improvement, the sputtered films were still the preferred ones because of the low cost and convenience in making them as well as the satisfactory reproducibility achievable. Although the low cost of the Au films makes the regeneration of sensor surfaces for repetitive measurements unnecessary, we denatured the duplexes at the Au films produced with the ion beam coater to investigate whether such a regeneration will further improve the precision. The denaturing step was carried out by soaking the films in a water bath with temperatures greater than the melting points of the duplexes. Unfortunately, signals arising from the rehybridization at the 'regenerated' sensor surfaces were found to deteriorate dramatically (by ≥ 60 –70% between two consecutive measurements). Thus, it appears that the use of the disposable sputtered Au films as the sensor is a more time-effective route for the SPR analysis.

In the lower concentration range, the slope of the plot in Figure 4 is more pronounced. This could be interpreted on the basis that, at a concentration < 0.36 pM, the injected samples contain targets present at a level far less than that for consuming the effective ODN probes [governed mainly by their orientations (30)]. At a higher target concentration, the effective probes can be quickly consumed in one to two injections. Thus, beyond a certain point (e.g. 1.2 pM), an increase in the target concentration will not significantly increase the SPR signal.

Similar to the probe immobilization process, the hybridization was also found to be instantaneous because an abrupt SPR dip shift was observed once the solution of the complementary target came in contact with the probe-covered Au surface. Perhaps the most noteworthy aspect is the remarkably low detection level achieved with our FI-SPR device. The amount

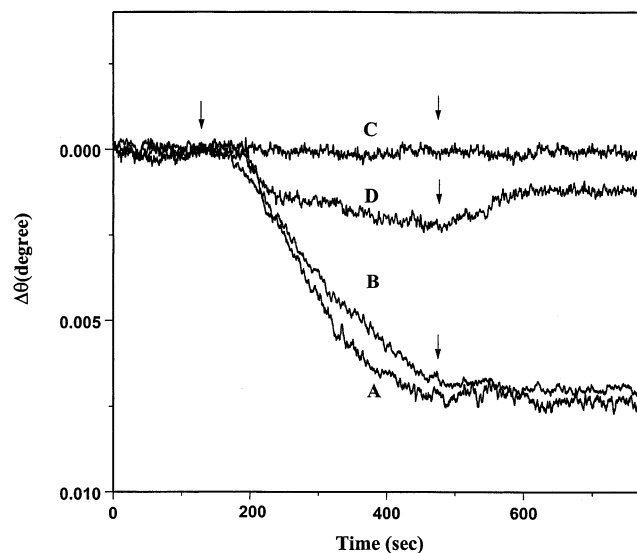


Figure 5. Time-resolved SPR responses of the 30mer HS-ODN probes to the injection of 100 μ l of (curve A) a solution containing 0.18 pM 47mer target DNA, (curve B) a mixed solution containing 0.18 pM 47mer target and 18 nM 47mer target with six mismatching bases, (curve C) a solution of 18 nM 47mer target with six mismatching bases and (curve D) a solution of 18 pM target with a single mismatch.

of ODN target that gave rise to the signal in Figure 3, curve B (100 μ l of 0.054 pM) corresponds to 5.4 amol or 96 fg of target DNA.

The sequence specificity of the FI-SPR instrument was also investigated. Figure 5 shows the SPR responses of the immobilized 30mer probes to the injections of a solution of its complementary 47mer target (0.18 pM, curve A), a solution of the same 47mer target (0.18 pM, curve B) mixed with 10^5 -fold excess of a 47mer target containing six mismatching bases (18 nM, curve B), a solution of only the 47mer target with six mismatching bases (18 nM, curve C) and a solution of a 47mer target with a single mismatch (18 pM, curve D). Curve C shows essentially no SPR dip shift, indicating that hybridization did not take place between the DNA probes and the six-base mutant. The absence of non-specific hybridization is further reflected by the fact that curves A and B exhibit virtually the same overall SPR dip shift. For the injection of the 47mer target with a single-base mismatch, a small SPR dip shift appeared once the injected sample entered the cell, apparently due to the duplex formation with one base-pair mismatch. This dip shift was offset to the baseline to some extent when the sample solution was replaced by the carrier solution (see arrows in the Figure, presumably due to the dissociation of the imperfectly matched duplexes). The net dip shift was found to be $\sim 17\%$ of the overall dip shift associated with duplex formation between the probe and complementary target (curve A). Since the experiment was conducted at room temperature, a decrease in the SPR signal by $> 80\%$ suggests that our FI-SPR is capable of performing sequence-specific analysis.

Sequence-specific gene analysis of the *A.thaliana* cDNA samples

To demonstrate the potential of our FI-SPR for label-free analysis of real samples, two representative genes in a cDNA

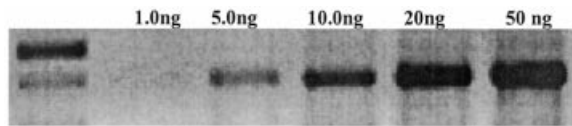


Figure 6. Analytical gel showing a linear correlation between amounts of RT-PCR product obtained and amounts of mRNA used for the cDNA preparation.

mixture derived from *A.thaliana* leaf extracts were quantified and the results were compared with more standard RT-PCR measurements.

In *A.thaliana*, the transition from vegetative growth to reproductive growth is associated with a drop in ascorbate peroxidase (APx) enzymatic activity in rosette leaves (57). The decline is accompanied by an increase in lipid peroxidation, apparently through the activation of a C13-specific lipoxygenase. Our current hypothesis is that the APx decline and subsequent activation of the octadecanoate pathway are early events leading to the eventual induction of senescence-associated genes. Thus, these events may comprise a portion of the signal transduction pathway that couples flowering time to leaf longevity. An accurate quantification of the amount of APx mRNA at the reproductive transition will allow us to elucidate the mechanism of the APx decline. To test whether this decline is due to a change in transcription of the APx genes, we conducted a relative RT-PCR quantification of the APx genes. *Arabidopsis thaliana* has five genes encoding APx (58). The products are found in the cytosol (cs1 and cs2), the chloroplast (cht and chs) and associated with the glyoxysome (cm1). Since significant APx changes occur at the enzyme level [up to 5-fold decline and subsequent rebound (57)], we decided to normalize APx mRNA levels to an invariant control message that encodes cytoskeletal actin. Figure 6 shows the dependence of APx-cs2 PCR product on the amount of starting total mRNA. The product first appeared with 5 ng of total mRNA in the reverse transcription reaction and increased linearly up to 50 ng of the starting mRNA. To measure the ratio of APx-cs2 mRNA to actin mRNA, we performed RT-PCR reactions at several cycle numbers to ensure that products were quantified in the linear range of the amplification process. The RT-PCR products are shown in Figure 7. Product yields for both messages were linear up to 25 cycles. At the midpoint in the linear range, the ratio of actin to APx-cs2 product was 1.8, with a threshold cycle number of 15 for appearance of the actin product and 20 for appearance of the APx-cs2 product.

While the aforementioned RT-PCR experiments estimated the ratio between the APx and actin genes, the ratio is semiquantitative at best because of the uncertainties involved in differential amplifications of different genes. Moreover, owing to the small leaf extract available for quantification and the extensive sample pretreatment and amplification, the procedure is relatively time consuming. To circumvent these problems, we carried out an FI-SPR analysis of the cDNA transcribed quantitatively from mRNA.

Curves A, B and C in Figure 8 are the SPR signals resulting from the injections of 33 pg/ml of total cDNA solutions (3.3 pg of total cDNA injected) into the flow cell housing Au films immobilized with the APx-cs2 probe, a 35mer probe

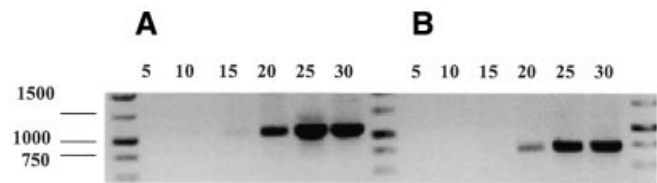


Figure 7. PCR kinetics of actin2 and APx-cs2 showing the correlation between the number of PCR cycles and the amount of product obtained. (A) The product of the actin2 primers. (B) The product of the APx-cs2 primers.

with one-base mismatch to the APx-cs2 gene and a probe with six mismatching bases, respectively. Notice that both curves B and C show the DNA duplex formation upon introducing the sample solution into the flow cell and the DNA duplex dissociation when the carrier solution replenishes the cell. With the six mismatching bases, essentially all the duplexes formed at the sensor surface can be completely dissociated. With the single-base mismatch (curve B), the net SPR dip shift (after the cell content has been completely replaced by the carrier solution) dropped by >60% at the Au surface. Such a large decrease in the SPR signal again indicates that there is a high degree of sequence specificity. It is interesting to note that the effect of single base mismatch on the ODN probe/target duplex formation (curve D in Fig. 5) appears to be more pronounced than that between the ODN probe and the cDNA polynucleotide target (curve B in Fig. 8) in that a larger dip shift was observed for the latter. This can be explained on the basis that the cDNA molecules, with much longer strands (756 versus 47 bases in the target ODN), lead to the formation of a thicker DNA film and consequently result in a greater SPR dip shift.

It is worth noting that, though the SPR signal arising from the APx hybridization (curve A of Fig. 8) is comparable with that from the 47mer hybridization (curve A of Fig. 5), the hybridization efficiency associated with the former is much smaller. The net SPR dip shift in curve A of Figure 8 corresponds to the hybridization of the cDNA with only 0.3% of the total probe molecules immobilized on the surface. This is in sharp contrast to the 7% deduced from curve A of Figure 5. This discrepancy can be easily understood on the basis that DNA targets with much longer strands encounter greater steric hindrance, inhibiting effective hybridization at the sensor/solution interface. The reduced hybridization efficiency due to the steric congestion of probes at a solid sensing surface has been observed in our previous studies (18,47) and noted by other research groups (32,59). Fortunately, our SPR is extremely sensitive to the thickness change occurring at the surface. Consequently, the much longer DNA strand would cause a greater SPR dip shift, offsetting the decrease in the hybridization efficiency to a large extent.

Finally, we analyzed the content of the actin cDNA by injecting the same cDNA solution into the flow cell housing a Au film covered with a probe whose sequence recognizes the actin gene (curve D in Fig. 8), in an attempt to gauge the ratio between the actin and APx products. The ratio deduced from the net SPR dip shifts in curves D and A, 1.3, is in good agreement with the ratio yielded by the RT-PCR experiment (Fig. 7). While this agreement validates our FI-SPR for real-

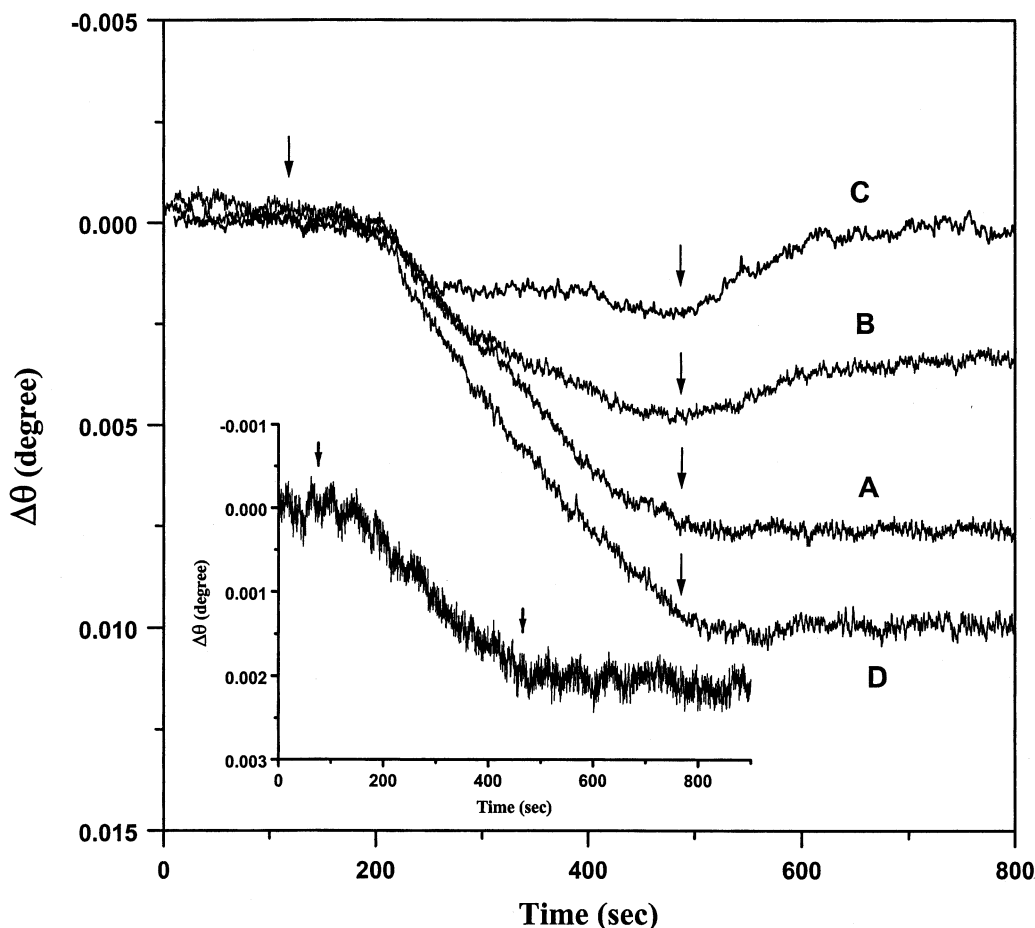


Figure 8. Time-resolved SPR response of a 35mer APx-cs2 probe (curve A) and a 35mer probe with one mismatching base to the APx-cs2 gene (curve B) to the injections of a sample containing 33 pg/ml of total cDNA. Curve C corresponds to the SPR responses of a 35mer probe with six bases mismatching to the APx-cs2 gene and curve D is the time-resolved SPR response of the actin probe to the same cDNA solution. The inset depicts the SPR response similar to that of curve A, except that a more diluted cDNA sample (3.3 pg/ml total DNA) was injected.

sample analysis, we should emphasize that the ratio provided by the SPR measurements should be more accurate, because our FI-SPR has a detection limit much lower than that of RT-PCR. In other words, the greater signal-to-noise ratio in our FI-SPR experiments provided more data fidelity. The satisfactory signal-to-noise ratio is reflected by the inset of Figure 8 which shows the SPR response to the injection of 0.33 pg of total cDNA. Clearly, the response permitted an easy quantification of the amount of APx-cs2 gene in the cDNA mixture. Such a detection limit is $>10^4$ -fold lower than that for the RT-PCR (5 ng of total mRNA in Fig. 6). The capability of our FI-SPR for the accurate analysis of unlabeled species in a complicated sample matrix is therefore advantageous and could be utilized for direct quantification of gene expression using very small quantities of other biological samples.

DISCUSSION

Hybridization efficiencies of immobilized HS-ODN probes with ODN targets and cDNAs

The surface coverage of HS-ODN probes (11%) and their hybridization efficiency (9%) agree with values reported

previously. Steel *et al.* (52) showed that the full surface coverage (calculated to be $\sim 6 \times 10^{13}$ molecules/cm²) cannot be obtained from a series of ODN probes. We and other research groups show that a variety of parameters [e.g. probe length (52), probe concentration (18), time used for the immobilization (54) and morphology of the Au surface (18)] are important factors for surface coverage and orientation of the probes which, in turn, govern the hybridization efficiency. Given the agreement of our FI-SPR results with other previously reported values, it appears that studies of the HS-ODN probe immobilization and hybridization serve well as a model system.

As described in connection with the description of the inset of Figure 3, only a small fraction (9%) of the probes are involved in duplex formation. Such low hybridization efficiencies are not unexpected, given the relatively disordered ODN surface orientations. Since it is well known that probes whose strands are not extended into the solution are not effective for hybridization at the surface/solution interface, different methods have been investigated to reorient the HS-ODN probes to increase the efficiency (18,48,53-55) or to conduct post-hybridization signal amplification to enhance the relatively weak analytical signals (19,21,29). Note that in

the present work, neither probe reorientation nor signal amplification was explored for the model system or the real-sample analysis. Thus, it is remarkable that, despite the fact that the HS-ODN probe orientation does not facilitate high hybridization efficiency, our SPR displays rather large signals for hybridizations with both ODN targets and cDNAs. We should point out that, by altering the probe surface density and orientation, the upper limit of the dynamic range shown in Figure 4 should be extendable to higher concentrations. Since the focus of this work is on the enhancement of the SPR sensitivity for ultratrace analysis and designing sensor surfaces optimal for a greater extent of hybridization has been developed by us and other research groups (18,48,52,55), we did not explore the SPR detection with DNA probes attached onto gold surfaces via other less straightforward immobilization schemes.

Detection levels for ODN targets and cDNAs

Perhaps the most attractive feature of our FI-SPR is the superb sensitivity to measure a very small SPR dip shift (10^{-4} – 10^{-5} degrees). Consequently the detection levels for the ODN targets and for cDNAs were both quite low. As demonstrated by Figure 3B (detection of 5.4 amol of a 47mer target) and inset of Figure 8 (0.33 pg of total cDNAs), such values are much lower than those of other scanning SPR instruments (nM) and imaging SPR devices (28,30–36,43) as well as those aided by signal amplification using DNA-capped gold nanoparticles (1–10 pM) (29,37). Moreover, the amount of target determined is also lower or comparable with that detectable using fluorophore-tagged (20 amol/cm²) and radiolabeled (100 fg) DNA targets (22,54,60,61). We attribute the high sensitivity to the incorporation of the differential detection of the reflected light between the bi-cell photodetector. In AFM, such photodetector detectors have been shown to be capable of measuring individual atoms or molecules at surfaces (62). In our application, such a detector is more than sufficient for precisely monitoring the fine movement of the sharp dark line (SPR dip shift) (46).

Sequence specificity

Similar to other instruments (18,20) and the various SPR devices (24,29,32,63), our FI-SPR results indicate that HS-ODN probes immobilized onto gold films possess an excellent sequence specificity toward both ODN and PDN (i.e. cDNA) targets. The comparison between curves A and C in Figure 5 shows that the 47mer target with the six-base mismatch did not hybridize with the 30mer HS-ODN probe on the Au film. The analogous responses of curves A and B also indicate that the presence of a 10^5 -fold excess six-base mutant in a mixture solution did not alter the hybridization of the perfectly complementary target. This implies that the association kinetics between the probe and its complementary target remained largely unchanged. While the SPR dip shift corresponding to the hybridization of the single-base mutant is more appreciable, the overall change is small (17% of the overall dip shift observed from the hybridization with the perfectly complementary target). Moreover, the much smaller signal and the small recovery of the SPR dip shift upon the completion of injection are consistent with other reports (20). The only limitation of the sequence-specific analysis based on our SPR approach might be that, when the

complementary target is present at a level much lower than the detection level and another DNA with a single mismatch is present at a much higher level, the observed SPR signal might be higher than the true value. However, situations like this would be rare because of the remarkably low detection level for the complement. To avoid potential misinterpretation of the data, one could conduct studies on the association and dissociation kinetics or perform the measurements at an elevated temperature (which will be somewhat challenging for the current instrumental design).

As for the selective detection of the genes (APx-cs2 and actin) in the cDNA mixture derived from the *A.thaliana* leaf extract, the behavior associated with the single-base and six-base mutant probes to the target hybridization exhibited a similar trend to their ODN counterparts (curves D and C in Fig. 5), again suggesting that sequence-specific DNA analysis can be accomplished with even more complex samples. As for more complicated cases where a mismatching long DNA strand is coexistent with a short complementary strand (i.e. the longer strand of the mismatching DNA might introduce a considerable 'false' signal), one could resolve the problem by judiciously choosing a probe of the appropriate length (59) or intermixing probes with other molecules [e.g. alkanethiols (18,48,52,55)]. It has been shown that the steric congestion introduced by immersing short probes in other species on the same sensor can dramatically limit the extent of hybridization of PDNs or DNA targets of relatively long strands (18,48,52,55,59).

Finally, it is worth mentioning that the universal oligo-dT primer was used for the reverse transcription of mRNA to cDNA and consequently several thousands of different mRNAs contained in the *A.thaliana* extract were converted to their corresponding cDNAs. Detection of specific target cDNA sequences in such a complex sample matrix is a serious challenge for many techniques. The fact that the sequence specificity for the real-sample analysis showed a similar trend to that of the model system and the consistency in the ratio of actin over APx-cs2 between the FI-SPR and these RT-PCR measurements both verify the capability of our FI-SPR for sequence-specific DNA analysis in cellular samples. Moreover, the superb sensitivity and the small sample consumption associated with the FI-SPR (as compared with methods such as northern blotting) allowed us to dilute samples significantly without greatly compromising the analytical signals or sample consumption. For the acquisition of the inset of Figure 8, 100 μ l of a sample diluted from the original extract by 10^5 -fold corresponds to 0.33 pg of total cDNAs. This feature should be attractive for the analysis of a species from very small biological samples.

CONCLUSION

A highly sensitive FI-SPR device for label-free sequence-specific ODN and PDN assays has been constructed. Through studying hybridization between a 35mer probe immobilized onto a Au surface and a 47mer target, the analytical performance of the resultant FI-SPR was established. A concentration detection level for the 47mer target at ~ 54 fM with the total amount of target of 5.4 amol can be detected. Such a value represents a decrease for the concentration detection level achievable with other SPR instruments of 2–3

orders of magnitude. Such a remarkable sensitivity also compares well with the commonly used sensitive techniques based on the detection of labeled DNA samples (e.g. fluorophore-tagged and radiolabeled targets). The selectivity of the SPR measurements at the DNA sensor surface was excellent, since the duplexes formed with single and six mismatching base pairs caused small or no appreciable SPR dip shifts. The possibility of extending this device for the analyses of real samples was demonstrated by selectively determining two specific genes in a cDNA mixture reverse transcribed from mRNAs in *A.thaliana*. We demonstrate that sequence-specific analysis of the unlabeled cDNA solutions at extremely low concentrations can be accomplished and our data can provide confirmative and complementary information to those obtained from other measurements (e.g. RT-PCR). The simplicity and the obviation of the labeling step make this device particularly attractive for the analysis of small amounts of DNA/RNA samples present in complex matrices.

ACKNOWLEDGEMENTS

We thank Dr S. Wang for his technical help. F.Z. and R.L.V. acknowledge support by the NIH-SCORE subproject (GM08101) and the NSF-CRUI program (DBI-9978806 for F.Z. and DBI-9710796 for R.L.V.) and N.T. thanks the donors of the Petroleum Research Fund (33516-AC5) administered by the ACS and NSF (CHE-9818073) for financial support.

REFERENCES

1. Watson,J., Gilman,M., Witkowski,J. and Zoller,M. (1992) *Recombinant DNA*, 2nd Edn. W.H.Freeman and Company, New York, NY.
2. Mullis,K.B., Ferre,F. and Gibbs,R.A. (1994) *The Polymerase Chain Reaction*. Birkhauser, Boston, MA.
3. Cottrez,F., Auriault,C., Capron,A. and Groux,H. (1994) Quantitative PCR: validation of the use of a multispecific internal control. *Nucleic Acids Res.*, **22**, 2712–2713.
4. Raeymaekers,L. (1993) Quantitative PCR: theoretical considerations with practical implications. *Anal. Biochem.*, **214**, 582–585.
5. Piuino,P.A.E., Knull,U.J., Hudson,R.H.E., Damha,M.J. and Cohen,H. (1995) Fiber-optic DNA sensor for fluorometric nucleic acid determination. *Anal. Chem.*, **67**, 2635–2643.
6. Fotin,A.V., Drobyshev,A.L., Proudnikov,D.Y., Perov,A.N. and Mirzabekov,A.D. (1998) Parallel thermodynamic analysis of duplexes on oligodeoxyribonucleotide microchips. *Nucleic Acids Res.*, **26**, 1515–1521.
7. Xu,X.-H., Yang,H.C., Mallouk,T.E. and Bard,A.J. (1994) Immobilization of DNA on an aluminum(III) alkanebisphosphonate thin film with electrogenerated chemiluminescent detection. *J. Am. Chem. Soc.*, **116**, 8386–8387.
8. Kelley,S.O., Barton,J.K., Jackson,N.M. and Hill,M.G. (1997) Electrochemistry of methylene blue bound to a DNA-modified electrode. *Bioconjug. Chem.*, **8**, 31–37.
9. Kelley,S.O., Boon,E.M., Barton,J.K., Jackson,N.M. and Hill,M.G. (1999) Single-based mismatch detection based on charge transduction through DNA. *Nucleic Acids Res.*, **27**, 4830–4837.
10. Wang,J., Xu,D., Kawde,A.-N. and Polsky,R. (2001) Metal nanoparticle-based electrochemical stripping potentiometric detection of DNA hybridization. *Anal. Chem.*, **73**, 5576–5581.
11. Wang,J., Rivas,G., Fernandez,J., Paz,J.L., Jiang,M. and Waymire,R. (1998) Indicator-free electrochemical DNA hybridization biosensor. *Anal. Chim. Acta*, **375**, 197–203.
12. Wang,J., Rivas,G., Ozsoz,M., Grant,D., Cai,X. and Parrado,C. (1997) Microfabricated electrochemical sensor for the detection of radiation-induced DNA damage. *Anal. Chem.*, **69**, 1457–1460.
13. Patolsky,F., Lichtenstein,A. and Willner,I. (2001) Electronic transduction of DNA sensing processes on surfaces: amplification of DNA detection and analysis of single-base mismatches by tagged liposomes. *J. Am. Chem. Soc.*, **123**, 5194–5205.
14. Furtado,L.M., Su,H., Thompson,M., Mack,D.P. and Hayward,G.L. (1999) Interactions of HIV-1 TAR RNA with tat-derived peptides discriminated by on-line acoustic wave detector. *Anal. Chem.*, **71**, 1167–1175.
15. Thompson,M. and Furtado,L.M. (1999) High density oligonucleotide and DNA probe arrays for the analysis of target DNA. *Analyst*, **124**, 1133–1136.
16. Furtado,L.M. and Thompson,M. (1998) Hybridization of complementary strand and single-base mutated oligonucleotides detected with an on-line acoustic wave sensor. *Analyst*, **123**, 1937–1945.
17. Wang,J. (2000) Survey and summary from DNA biosensors to gene chips. *Nucleic Acids Res.*, **28**, 3011–3016.
18. Huang,E., Satiapipat,M., Han,S. and Zhou,F. (2001) Surface structure and coverage of an oligonucleotide probe tethered onto a gold substrate and its hybridization efficiency for a polynucleotide target. *Langmuir*, **17**, 1215–1224.
19. Han,S., Lin,J., Satiapipat,M., Baca,A.J. and Zhou,F. (2001) A three-dimensional heterogeneous DNA sensing surface formed by attaching oligonucleotide-capped gold nanoparticles onto a gold-coated quartz crystal. *Chem. Commun.*, **7**, 609–610.
20. Okahata,Y., Kawase,M., Niikura,K., Ohtake,F., Furusawa,H. and Ebara,Y. (1998) Kinetic measurements of DNA hybridization on an oligonucleotide-immobilized 27-MHz quartz crystal microbalance. *Anal. Chem.*, **70**, 1288–1296.
21. Patolsky,F., Lichtenstein,A. and Willner,I. (2000) Amplified microgravimetric quartz-crystal-microbalance assay of DNA using oligonucleotide-functionalized liposomes or biotinylated liposomes. *J. Am. Chem. Soc.*, **122**, 418–419.
22. Pang,H.-M. and Yueng,E.S. (2000) Automated one-step DNA sequencing based on nanoliter reaction volumes and capillary electrophoresis. *Nucleic Acids Res.*, **28**, e73.
23. Silin,V. and Plant,A. (1997) Biotechnological applications of surface plasmon resonance. *Trends Biotechnol.*, **15**, 353–359.
24. Plant,A.L., Brighamburke,M., Petrella,E.C. and Oshannessy,D.J. (1995) Phospholipid/alkanethiol bilayers for cell-surface receptor studies by surface plasmon resonance. *Anal. Biochem.*, **226**, 342–348.
25. Yang,M., McGovern,M.E. and Thompson,M. (1997) Genosensor technology and the detection of interfacial nucleic acid chemistry. *Anal. Chim. Acta*, **346**, 259–275.
26. Brockman,J.M., Nelson,B.P. and Corn,R.M. (2000) Surface plasmon resonance imaging measurements of ultrathin organic films. *Annu. Rev. Phys. Chem.*, **51**, 41–63.
27. Georgiadis,R., Peterlinz,K.P. and Peterson,A.W. (2000) Quantitative measurements and modeling of kinetics in nucleic acid monolayer films using SPR spectroscopy. *J. Am. Chem. Soc.*, **122**, 3166–3173.
28. Heaton,R.J., Peterson,A.W. and Georgiadis,R.M. (2001) Electrostatic surface plasmon resonance: direct electric field-induced hybridization and denaturation in monolayer nucleic acid films and label-free discrimination of base mismatches. *Proc. Natl Acad. Sci. USA*, **98**, 3701–3704.
29. He,L., Musick,M.D., Nicewarner,S.R., Salinas,F.G., Benkovic,S.J., Natan,M.J. and Keating,C.D. (2000) Colloidal Au-enhanced surface plasmon resonance for ultrasensitive detection of DNA hybridization. *J. Am. Chem. Soc.*, **122**, 9071–9077.
30. Peterlinz,K.A., Georgiadis,R.M., Herne,T.M. and Tarlov,M.J. (1997) Observation of hybridization and dehybridization of thiol-tethered DNA using two-color surface plasmon resonance spectroscopy. *J. Am. Chem. Soc.*, **119**, 3401–3402.
31. Peterson,A.W., Heaton,R.J. and Georgiadis,R. (2000) Kinetic control of hybridization in surface immobilized DNA monolayer films. *J. Am. Chem. Soc.*, **122**, 7837–7838.
32. Nelson,B.P., Grimsrud,T.E., Liles,M.R., Goodman,R.M. and Corn,R.M. (2001) Surface plasmon resonance imaging measurements of DNA and RNA hybridization adsorption onto DNA microarrays. *Anal. Chem.*, **73**, 1–7.
33. Kai,E., Sawata,S., Ikenbukuro,K., Iida,T., Honda,T. and Karube,I. (1999) Detection of PCR products in solution using surface plasmon resonance. *Anal. Chem.*, **71**, 796–800.
34. Gotoh,M., Hasegawa,Y., Shinohara,Y., Shimizu,M. and Tosu,M. (1995) A new approach to determine the effect of mismatches on kinetic

- parameters in DNA hybridization using an optical biosensors. *DNA Res.*, **2**, 285–293.
35. Piscevic, D., Lawall, R., Veith, M., Liley, M., Okahata, Y. and Knoll, W. (1995) Oligonucleotide hybridization observed by surface plasmon optical techniques. *Appl. Surf. Sci.*, **90**, 425–436.
 36. Bates, P.J., Dosanjh, H.S., Kumar, S., Jenkins, T.C., Laughton, C.A. and Neidle, S. (1995) Detection and kinetic studies of triplex formation by oligodeoxynucleotides using real-time biomolecular interaction analysis (BIA). *Nucleic Acids Res.*, **23**, 3627–3632.
 37. Lyon, L.A., Musick, M.D. and Natan, M.J. (1998) Colloidal Au-enhanced surface plasmon resonance immunosensing. *Anal. Chem.*, **70**, 5177–5183.
 38. Lyon, L.A., Musick, M.D., Smith, P.C., Reiss, B.D., Pena, D.J. and Natan, M.J. (1999) Surface plasmon resonance of colloidal Au-modified gold films. *Sensors and Actuators B*, **54**, 118–124.
 39. Jung, L.S., Shumaker-Parry, J.S., Campbell, C.T., Yee, S.S. and Gelb, M.H. (2000) Quantification of tight binding to surface-immobilized phospholipid vesicles using surface plasmon resonance: binding constant of phospholipase A2. *J. Am. Chem. Soc.*, **122**, 4177–4184.
 40. Wink, T., van Zuilen, S.J., Bult, A. and van Bennekom, W.P. (1998) Liposome-mediated enhancement of the sensitivity in immunoassays of proteins and peptides in surface plasmon resonance spectrometry. *Anal. Chem.*, **70**, 827–832.
 41. Rao, J., Yan, L., Xu, B. and Whitesides, G.M. (1999) Using surface plasmon resonance to study binding of vancomycin and its dimer to self-assembled monolayers presenting D-Ala-D-Ala. *J. Am. Chem. Soc.*, **121**, 2629–2630.
 42. Ramsay, G. (ed.) (1998) *Commercial Biosensors: Applications to Clinical, Bioprocess and Environmental Samples*. John Wiley and Sons, Inc., New York, NY.
 43. Persson, B., Stenhag, K., Nilsson, P., Larsson, A., Uhlen, M. and Nygren, P.A. (1997) Analysis of oligonucleotide probe affinities using surface plasmon resonance: a means for mutational scanning. *Anal. Biochem.*, **246**, 34–44.
 44. Kubitschko, S., Spinke, J., Bruckner, T., Pohl, S. and Oranth, N. (1997) Sensitivity enhancement of optical immunosensors with nanoparticles. *Anal. Biochem.*, **253**, 112–122.
 45. Boussaad, S., Pean, J. and Tao, N.J. (2000) High-resolution multiwavelength surface resonance spectroscopy for probing conformational and electronic changes in redox proteins. *Anal. Chem.*, **72**, 222–226.
 46. Tao, N.J., Boussaad, S., Huang, W.L., Arechabaleta, R.A. and D'Agness, J. (1999) High resolution surface plasmon resonance spectroscopy. *Rev. Sci. Instrum.*, **70**, 4656–4660.
 47. Han, S., Lin, J., Zhou, F. and Vellanoth, R.L. (2000) Oligonucleotide-capped gold nanoparticles for improved atomic force microscopic imaging and enhanced selectivity in polynucleotide detection. *Biophys. Biochem. Res. Commun.*, **279**, 265–269.
 48. Satjapipat, M., Sanedrin, R. and Zhou, F. (2001) Selective desorption of alkanethiols in mixed self-assembled monolayers for subsequent oligonucleotide attachment and DNA hybridization. *Langmuir*, **17**, 7637–7644.
 49. Okahata, Y., Matsunobu, Y., Ijiro, K., Mukae, M., Murakami, A. and Mikano, K. (1992) Hybridization of nucleic acids immobilized on a quartz crystal microbalance. *J. Am. Chem. Soc.*, **114**, 8299–8300.
 50. Thiel, A.J., Frutos, A.G., Jordan, C.E., Corn, R.M. and Smith, L.M. (1997) *In situ* surface plasmon resonance imaging detection of DNA hybridization to oligonucleotide arrays on gold surfaces. *Anal. Chem.*, **69**, 4948–4956.
 51. Watts, H.J., Yeung, D. and Parkes, H. (1995) Real-time detection and quantification of DNA hybridization by an optical biosensor. *Anal. Chem.*, **67**, 4283–4289.
 52. Steel, A.B., Levicky, R.L., Herne, T.M. and Tarlov, M.J. (2000) Immobilization of nucleic acids at solid surfaces: effect of oligonucleotide length on layer assembly. *Biophys. J.*, **79**, 975–981.
 53. Steel, A.B., Herne, T.M. and Tarlov, M.J. (1998) Electrochemical quantification of DNA immobilized on gold. *Anal. Chem.*, **70**, 4670–4677.
 54. Levicky, R., Herne, T.M., Tarlov, M.J. and Satija, S.K. (1998) Using self-assembly to control the structure of DNA monolayers on gold: a neutron reflectivity study. *J. Am. Chem. Soc.*, **120**, 9787–9792.
 55. Herne, T.M. and Tarlov, M.J. (1997) Characterization of DNA probes immobilized on gold surfaces. *J. Am. Chem. Soc.*, **119**, 8916–8920.
 56. Skoog, D.A., Holler, F.J. and Nieman, T.A. (1998) *Principles of Instrumental Analysis*. Saunders College Publishing, Philadelphia, PA.
 57. Ye, Z., Rodriguez, R., Tran, A., Hoang, H., de los Santos, D., Brown, S. and Vellanoth, R. (2000) The developmental transition to flowering represses ascorbate peroxidase activity and induces enzymatic lipid peroxidation in leaf tissue in *Arabidopsis thaliana*. *Plant Sci.*, **158**, 115–127.
 58. Jespersen, H.M., Kjaersgard, I.V., Ostergaard, L. and Welinder, K.G. (1997) From sequence analysis of three novel ascorbate peroxidases from *Arabidopsis thaliana* to structure, function and evolution of seven types of ascorbate peroxidase. *Biochem. J.*, **326**, 305–310.
 59. Demers, L.M., Mirkin, C.A., Mucic, R.C., Reynolds, R.A., III, Letsinger, R.L., Elgahanian, R. and Viswanadham, G. (2000) A fluorescence-based method for determining the surface coverage and hybridization efficiency of thiol-capped oligonucleotides bound to gold thin films and nanoparticles. *Anal. Chem.*, **72**, 5535–5541.
 60. Duggan, D.J., Bittner, M., Chen, Y., Meltzer, P. and Trent, J.M. (1999) Expression profiling using cDNA microarrays. *Nature Genet. (Suppl.)*, **21**, 10–14.
 61. Schwarz, T., Yeung, D., Hawkins, E., Heaney, P. and McDougall, A. (1991) Detection of nucleic acid hybridization using surface plasmon resonance. *Trends Biotechnol.*, **9**, 339–340.
 62. Magonov, S.N. and Whangbo, M.-H. (1996) *Surface Analysis with STM and AFM*. VCH Publishers, Inc., New York, NY.
 63. Lyon, L.A., Holliday, W.D. and Natan, M.J. (1999) An improved surface plasmon resonance imaging apparatus. *Rev. Sci. Instrum.*, **70**, 2076–2081.